INTERNATIONAL JOURNAL OF HYDROGEN ENERGY 46 (2021) 10653–10665

Available online at www.sciencedirect.com

ScienceDirect

journal homepage: www.elsevier.com/locate/he

A grey wolf optimized fuzzy logic based MPPT for shaded solar photovoltaic systems in microgrids

Bhukya Laxman[*], *Anil Annamraju*, *Nandiraju Venkata Srikanth*

Department of Electrical Engineering, National Institute of Technology, Warangal, Telangana, 506004, India

HIGHLIGHTS

- A new MPPT using Grey Wolf optimized adaptive fuzzy logic controller is proposed.
- Grey Wolf optimization is used for tuning the scaling factors of MFs of FLC.
- The objective of the optimization of scaling factors is for better MPPT.
- The test system is examined under different shading patterns.
- It improves global MPP tracking speed and efficiency of solar PV system.

ARTICLE INFO

Article history:
Received 31 August 2020
Received in revised form
19 October 2020
Accepted 21 December 2020
Available online 19 January 2021

Keywords:
Grey wolf optimization
Solar photovoltaic system
Adaptive fuzzy logic controller
Maximum power point tracker
Partial shading condition

ABSTRACT

As the solar PV system (SPVS) suffered from an unavoidable complication that it has nonlinearity in I–V curves, the optimum maximum power point (MPP) measurement is difficult under fluctuating climatic conditions. For maximizing SPVS output power, MPP tracking (MPPT) controllers are used. In this paper, a new adaptive fuzzy logic controller (AFLC) based MPPT technique is proposed. In this proposed AFLC, the membership functions (MFs) are optimized using the Grey Wolf Optimization (GWO) technique to generate the optimal duty cycle for MPPT. Four shading patterns are used to experiment with the performance of the proposed AFLC. The proposed approach tracks the global MPP for all shading conditions and also enhances the tracking speed and tracking efficiency with reduced oscillations. The effectiveness and robustness of proposed AFLC based tracker results over P&O and FLC are validated using Matlab/Simulink environment. The proposed AFLC overcome the drawbacks of the classical P&O, and FLC approaches.

Introduction

Due to the conventional sources limitations and the issues of environment, the world is motivating towards renewable energy (RE) based microgrid system development. Microgrids are the systems consists of micro-sources, loads, storage systems with at least one distributed generation (DG) source and should be operated in grid-connected or islanded modes [1–3]. Microgrids offer enhanced local reliability, curtailed feeder losses, increased efficiency, and deliver uninterruptible supply function to the consumers [4,5]. The commonly used DG sources in microgrids are wind and solar for the reason that these are sustainable sources, ecologically friendly, and should be constructed at the utility or consumer side [6,7]. Out

* *Corresponding author.*
E-mail addresses: blaxman@student.nitw.ac.in (B. Laxman), ani223kumar@gmail.com (A. Annamraju), nvs@nitw.ac.in (N.V. Srikanth).
https://doi.org/10.1016/j.ijhydene.2020.12.158

of various RE sources, solar energy became the primary alternative source because it can be harnessed in all areas and is available every day. It became a leading renewable source due to its simple structure, having less pollution, less or zero-carbon greenhouse emission, and less maintenance cost. Currently, solar power is the envisaged alternative source by the world [8]. Nevertheless, the solar PV system (SPVS) suffered from an unavoidable complication that it has nonlinearity among the current and voltage predominantly under partially shaded conditions (PSC). In addition to PSCs, SPVS is affected by climatic conditions viz. hazy atmosphere and forest fire. The authors assessed the analysis of haze impact on solar PV systems. The haze particles prevent solar irradiance to reach PV panels which leads to a reduction in PV power. There are 15–20 hazy days for every year. The average PV power loss during the haze period is around 18% compared to a normal day [9]. Forest fires can play a vital role in climate change. During the forest fires period, the haze and smoke effects as pollution on the light intensity. Hence, SPVS has a power loss of up to 12.5% [10]. The authors also presented the works on the improvement of photocatalytic performance to utilize the enhanced visible light [11–13]. As the solar PV electrical characteristics having nonlinearity, optimum performance measurement assurance is not possible for fluctuating climatic conditions. To maximize SPVS output under fluctuating climate conditions, solar PV systems take account of MPPT controllers. These MPPT techniques use dc-dc converters for continuous MPP tracking.

A study of partial shadowing effects on SPVS characteristics for non-uniform insolation is designed in Ref. [14]. Based on this, G. Lijun et al. [15] proposed the construction of a series and parallel combination of SPVS and their MPP tracking. The comparison of many conventional MPPT techniques is presented [16,17]. Such techniques are hill-climbing/P&O, fractional open circuit voltage, fractional short circuit current, incremental conductance (INC), ripple correlation control (RCC) and these controllers could fails global MPP tracking. The P&O technique functions by perturbing voltage, and it has poor tracking time with constant vacillation at MPP [18]. Owing to the fact the INC method is commonly used because of easy implementation and enhanced efficiency. It functions based on the value of derivation of power against voltage presence positive on the left of MPP, zero at MPP, and negative on the right of MPP. The drawback of INC is a slow tracking time to reach MPP [16]. RCC takes converter signals to ripple to achieve the optimal point of MPP with the variation of operating current according to its location. It enhances tracking time but poorer MPP accuracy than other MPPTs.

The author in Ref. [19] proposed an FLC to track MPP and elevated the drawbacks of the P&O search method that the performance of FLC is fast converging and accurate tracking. The PV system has been tested for changing temperature and insolation levels [20,21] using FLC. Also compared the results for various performance parameters that are response time and tracking efficiency over conventional P&O. Jaw-KuenShiau et al. [22] presented the investigation on the design of FLC algorithms for solar MPPT using multiple fuzzy input variables. Some research works [23–25] conceded MPP tracking using the FLC technique by adding an extra gain block to the fuzzy system to tune the output. This drawback has been removed, and the duty cycle is achieved directly using the fuzzy rule-based system [26]. Moreover, this algorithm tracks MPP with expedient speed and better response for abrupt change with special conditions. The FLCs commonly used are built using type 1 fuzzy sets that have complications in diminishing the effect of uncertainties. Type 2 FLC [27] reduces this effect of uncertainties. Neural network-based MPP [28] tracking claims that enhanced efficiency over the FLC technique.

In this work, Grey Wolf optimized adaptive fuzzy logic controlled approach is proposed to extract the global MPP. The objective is to improve the efficiency and GMPP tracking of SPVS in all uniform and non-uniform irradiances. In proposed AFLC, Grey Wolf optimization (GWO) technique used for tuning the scaling factors of MFs of FLC. The objective of the optimization of scaling factors is to achieve quick response and reduce the steady state error. To exhibit the effectiveness and robustness of AFLC based tracker, results are validated using Matlab Simulink.

The leftover of this paper is summarized as follows: the next section describes the modeling of SPVS and its characteristics under PSC. And section 3 provides the gestalt of FLC approach to track MPPT. In Section 4 the proposed AFLC and GWO algorithm to optimize the FLC parameters are presented. The results and discussions with the performance of Proposed AFLC are shown in section 5. Finally, the last section provides conclusions.

Solar PV system under PSCs

PV cell model

The conventional single diode electrical model of PV cell comprises a light-current with an anti-parallel diode, one resistor in shunt, and a resistor in series across the load [29,30] shown in Fig. 1.

Applying KCL, The PV cell output current, I_{PV_C} obtained as:

$$I_{PV\_C} = I_{L\_C} - I_d - \frac{V_{PV\_C} + R_s * I_{PV\_C}}{R_{sh}} \quad (1)$$

where I_{L_C} is light produced current, I_d is diode current. The light-current, I_{L_C} of a PV cellbe subject to insolation and temperature is expressed as:

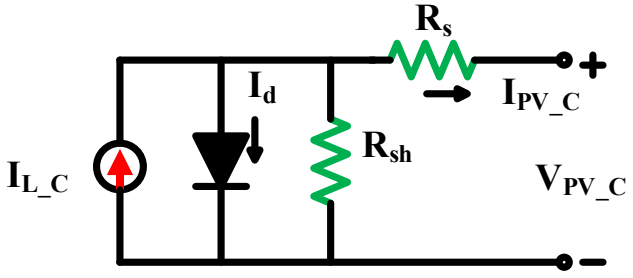

Fig. 1 – Electrical model of PV cell.

$$I_{L\_C} = \frac{G}{G_{ref}}\left[I_{L\_Cref} + \mu_{sc}\left(T_{cell} - T_{ref}\right)\right] \quad (2)$$

Also the diode current, I_d is;

$$I_d = I_o\left(e^{\frac{V_{PV\_C}+R_s * I_{PV\_C}}{V_t}} - 1\right) \quad (3)$$

The Io, diode saturation dark current is proportional to temperature can be obtained as:

$$I_o = I_{o,ref}\left(\frac{T_{cell}}{T_{ref}}\right)^3 \exp\left[\left(\frac{q\varepsilon_G}{A.K}\right)\left(\frac{1}{T_{ref}} - \frac{1}{T_{cell}}\right)\right] \quad (4)$$

PV module model

By and large, a PV cell generates a lesser amount of power less than 2 W. To enhance more power generation, the PV cells are configured as series-parallel [SP] combination. This SP combination of PV cells is termed as PV module. Thus a PV module consists Np cells in parallel and Ns cells in series depicted in Fig. 2. As a result, The PV module output current, I_{PV_M} obtained as:

$$I_{PV\_M} = N_p I_{L\_M} - N_p I_o\left[\exp\left(\frac{V_{PV\_M} + I_{PV\_M} * R_s \Lambda}{N_s V_t}\right) - 1\right] - \frac{V_{PV\_C} + \Lambda R_s * I_{PV\_C}}{\Lambda R_{sh}} \quad (5)$$

where,

$$\Lambda = \frac{N_s}{N_p} \quad (6)$$

SPVS under PSC

The SPVS is a solar array which is comprised of PV modules arranged in SP manner to come across energy demand. The choice of SP arrangement of modules in an array depends on factors that are PV material, performance, complexity, and energy demand. A common abnormal condition occurs in a PV array due to environmental conditions is called partial shadowing. To demonstrate SPVS under PSCs and its significance effects, a string of three modules (3S) in series with four different types of shading patterns is considered. The representation of 3S configuration with blocking and the by-pass diode is depicted in Fig. 3. The diodes are blocking, and by-pass is used to protect the module and to prevent "current reversal" and "hotspot" formation. Moreover, in uniform illuminated SPVS, the individual I–V curves added up and gives the only peak in the P–V curve. Further, the non-uniform illuminated modules in SPVS causes to produce multiple peaks in V–P curves. In this work different shading patterns considered, that are pattern 1: 1000, 1000, and 1000 w/m^2, pattern 2: 1000, 1000, and 500 w/m^2, pattern 3: 1000, 800, and 800 w/m^2, and pattern 4: 700, 800, and 600 w/m^2. Fig. 4 (a) and (b) shows V–I and V–P characteristics of SPVS under PSCs.

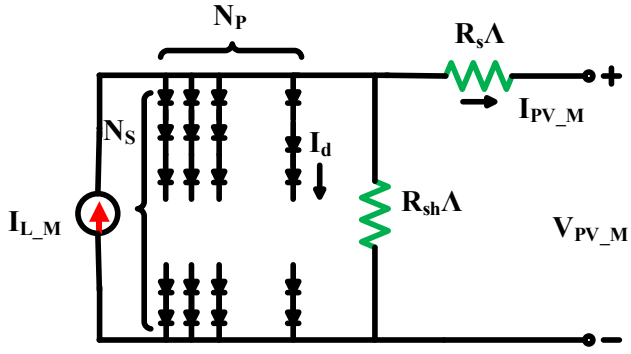

Fig. 2 – PV module.

Fuzzy logic based MPPT controller

The FLC method and conventional MPPTs are trapped at local MPP (LMPP) under shaded conditions. For avoiding LMPP tracking, a technique proposed [3] which has scan, store, perturb, and observe the operating power of the SPVS shown in Fig. 5 and flow chart shown in Fig. 6. This method tracks MPP under any climatic conditions, exclusively partially shadowing where global and local MPPs occur. For the period of initial state and fluctuating climatic conditions, it allows a wide range of search for scanning and storing the MPP value. A predetermined value that signifies the acceptable difference among the operating power and the recognized maximum power is stored to choose the controller rules. The duty cycle increases, if this difference among these two powers is higher than the predetermined value; or else, FLC based MPPT is applied. In this case, global MPP (GMPP) recovers quickly from fluctuating climatic conditions.

The FLC based MPPT using scan and the stored procedure designed for rapidly recover the global MPP. The FLC is formulated using MFs with input variables defined in Eqs. (7)–(9) are:

$$\Delta I = I(k) - I(k-1) \quad (7)$$

$$\Delta P = P(k) - P(k-1) \quad (8)$$

$$\Delta P_M = P_m(k) - P(k) \quad (9)$$

And the output variable is;

$$\Delta D = D(k) - D(k-1) \quad (10)$$

where ΔI and ΔP denotes the change in output current and change in output power of PV array, respectively, ΔP_M is the difference between stored peak power (*Pm*) and currently operated power, and ΔD is the change in duty cycle. Table 1 shows the fuzzy rules in which the two input variables, ΔI andΔP, and the output variable ΔD distributed into five fuzzy subsets expressed in linguistic labels. The input variable, ΔP_M is distributed into two linguistic variables that are PS and PL. The membership function for linguistic labels of input and output variables presented in Fig. 7. To work the fuzzy combination, Min-max method of Mamdani used. The ending stage of FLC is the defuzzification where the fuzzy singleton output transformed into an equal crisp control value [31]. Here the center of area method is used for the defuzzification.

The defuzzified output denoted as:

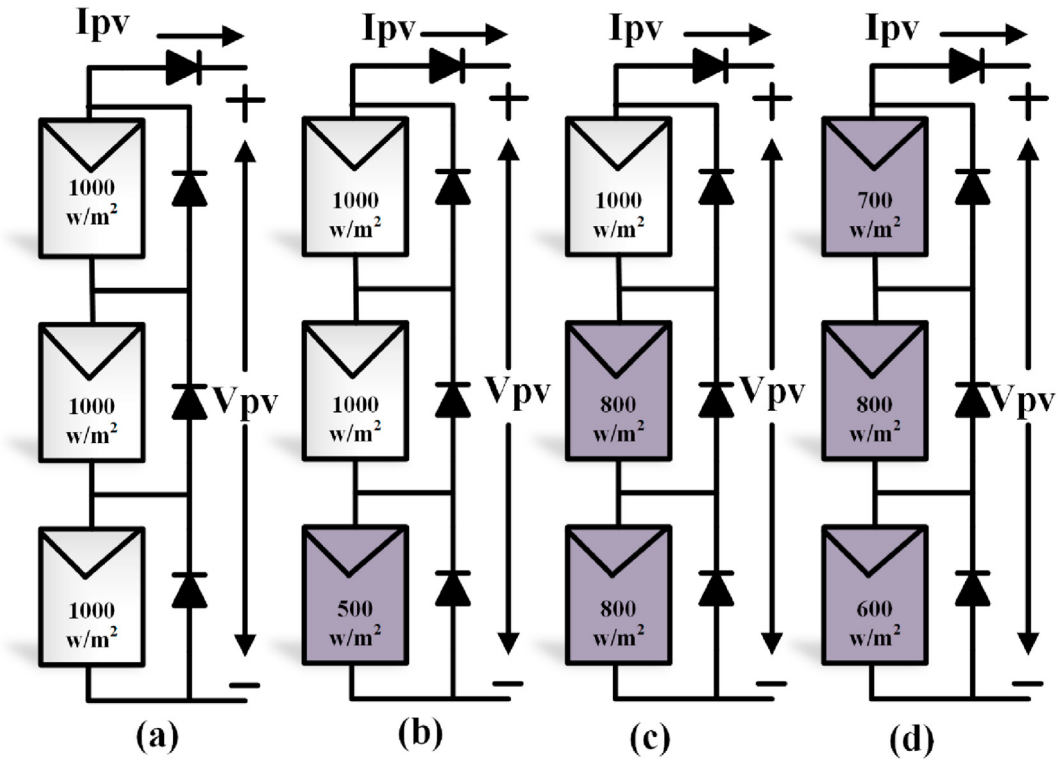

Fig. 3 – 3S configuration of SPVS with different shading patterns (a) Pattern1: 1000, 1000, and 1000 w/m². (b) Pattern2: 1000, 1000, and 500 w/m². (c) Pattern3: 1000, 800, and 800 w/m². (d) Pattern4: 700, 800, and 600 w/m².

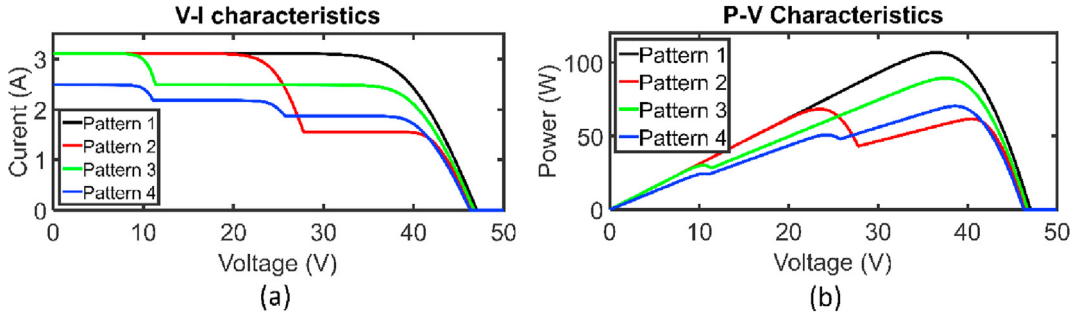

Fig. 4 – (a) The V–I curves of SPVS for different Shading patterns and (b) The V–P curves of SPVS for various shading patterns.

$$\Delta D = \frac{\sum_j^n \varepsilon(D_j) D_j}{\sum_j^n D_j} \tag{11}$$

where ΔD, the change is in duty cycle is an output of FLC, and D_j denotes the center of max-min method composition at the output MF.

Adaptive fuzzy logic based MPPT controller

The increasing complexity of MPPT tracking under partial shading conditions needs an accurate and fast tuning of control parameters for a better MPPT tracking. In light of this issue, in literature, authors proposed various optimization techniques for MPPT tracking. The inherent features of these algorithms are; independent on the model of the plant and derivative-free. Few of them like ACO, GA and PSO. According to theorem, no single Meta heuristic technique is suitable for solving all engineering optimization problems and scope of improvement is always persists [32–35]. Due to advantages in fast convergence, easy implementation structure, less number of controlling parameters and simplicity the GWO successfully implemented to various engineering problems. By considering this as motivation, a recently developed and powerful GWO is presented for accurate MPPT tracking.

The conventional FLC may produce some depicts due to improper selection of MFs. To improve the performance of FLC, the scaling factors of inputs and output parameters of FLC are optimized using swarm techniques. There are many approaches to tune fuzzy parameters [32–35]. In this, based on requirements and complexity of MPPT of SPVS, a novel

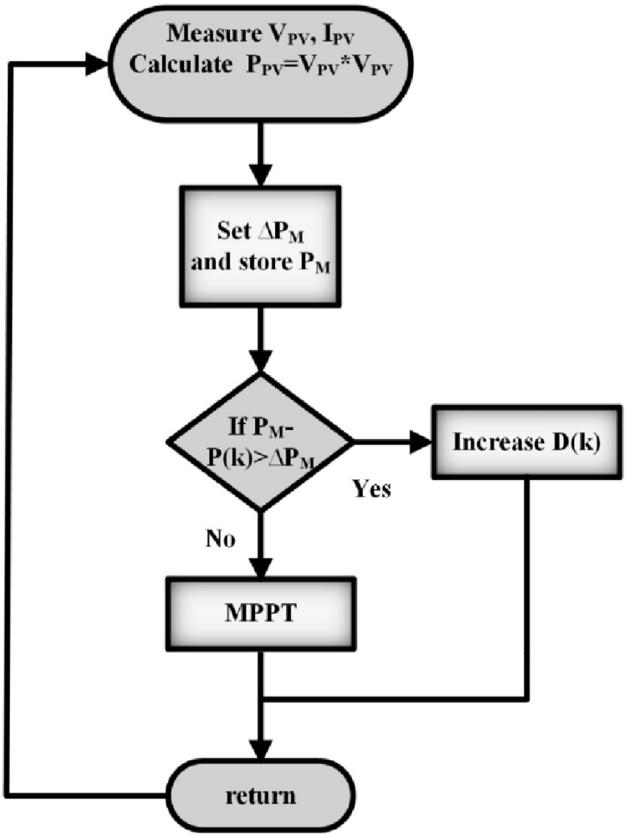

Fig. 5 – Solar PV system with MPPT controller.

Grey Wolf optimization (GWO) technique used for tuning the scaling factors of MFs of FLC. S. Mirjalili et al. [36] presented the detailed explanation of GWO. The erection of the proposed controller is depicted in Fig. 8. The reason for tuning of scaling factors of MFs instead of fuzzy set ranges is the number of variables for optimization is reduced [31]. The objective of the optimization of scaling factors is to achieve quick response and reduce the steady state error. The integral time absolute error (ITAE) criteria are used for the cost function and expressed as:

Table 1 – Fuzzy logic Rules.

ΔP	ΔI					
	NL	NS	ZE	PS	PL	ΔP_M
NL	ZE	ZE	NL	NL	NL	PS
NS	ZE	ZE	NS	NS	NS	
ZE	NS	ZE	ZE	ZE	PS	
PS	PS	PS	PS	ZE	ZE	
PL	PL	PL	PL	ZE	ZE	
NL	PB					PB
NS						
ZE						
PS						
PL						

$$ITAE = \int_0^\infty t^*|e(t)|dt \tag{12}$$

Grey Wolf Optimization

GWO was developed by Mirjali et al., in 2015, which mimics the collective behavior of grey wolves [36]. In general, grey wolves preferred to live in a pack consist of 5–12 wolves, and they have a strict dominant hierarchy presented in Fig. 9. Based on the ability to hunt the prey, the grey wolves are classified into four categories viz. alpha, beta, delta, and omega. The Alpha wolves are leaders in the pack, and they can be male or female, who are responsible for making decisions regarding sleeping place, time to wake, migration, hunting, and so on. All the wolves in the pack strictly follow the orders of the alpha wolf (dominant wolf). The only alpha wolves in the pack are allowed for mating. In general, the alpha wolves

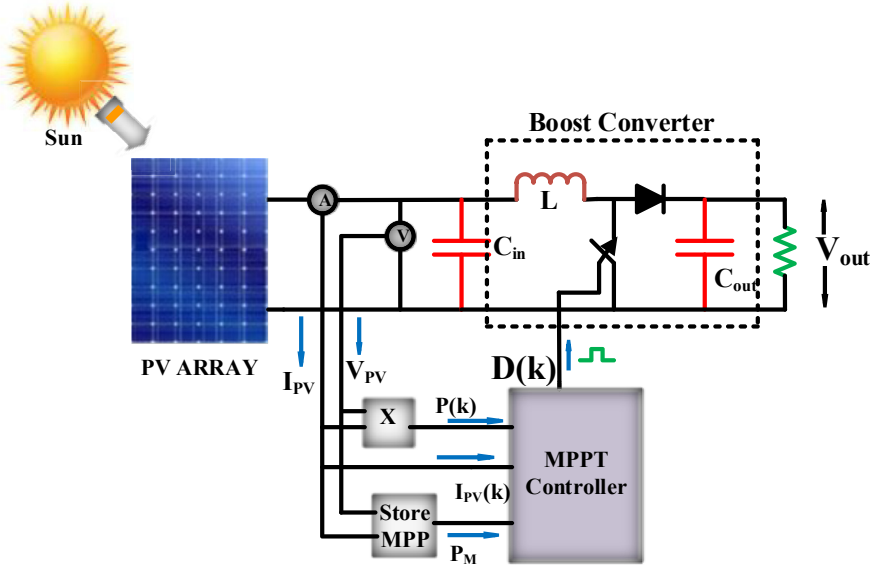

Fig. 6 – Flow chart.

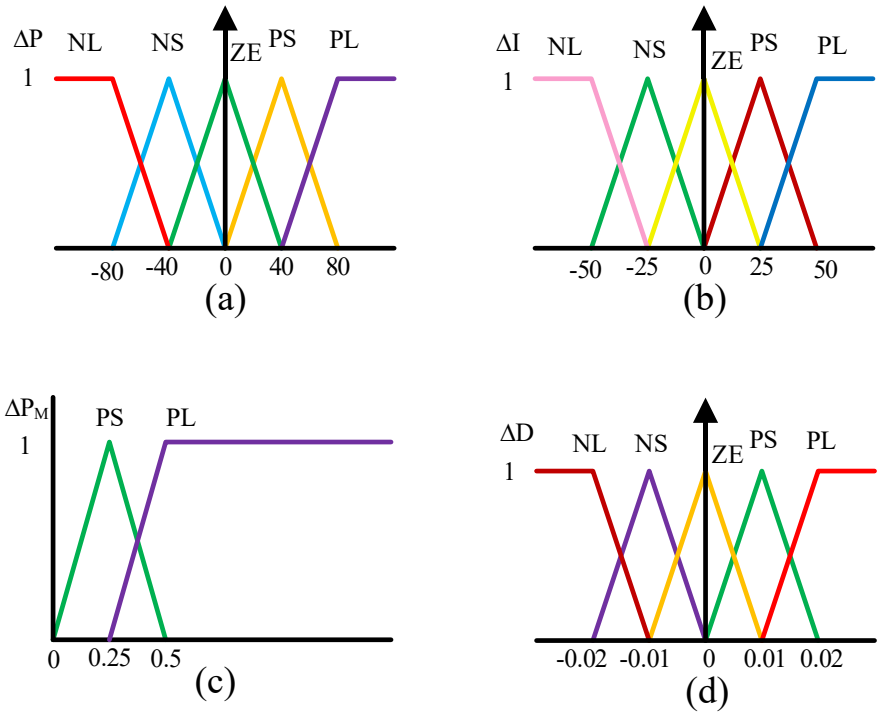

Fig. 7 – Fuzzymembership functions: (a) input ΔP (b) input ΔI (c) input ΔP_M, and (d) output ΔD.

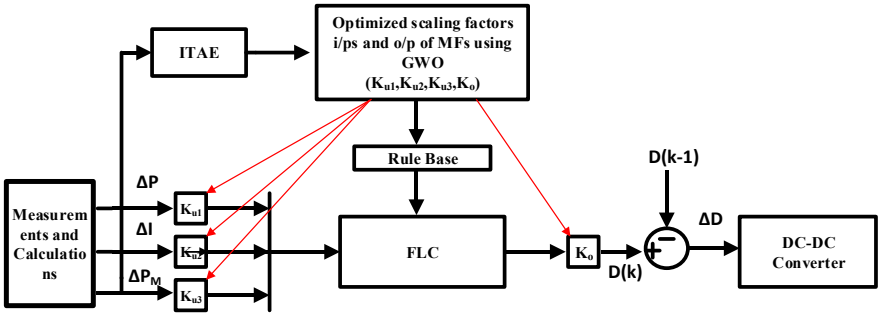

Fig. 8 – Block diagram proposed FLC.

are very efficient in managing the pack, but they may not be the fittest member of the grey wolf pack. It means that the discipline and organization of the grey wolf pack are most important compared to their strengths.

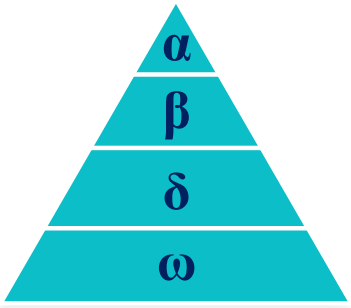

Fig. 9 – Grey wolf's hierarchy (dominance increasing from down to top).

The beta wolves are in the second level of the hierarchy, and they can assist and help alpha wolves in making the decisions and other activities in the pack. These beta wolves lead the pack when the alpha wolf passes away or becomes old. In this case, the betas command the other lower-level wolves, but they should respect the alpha. They play a disciplinary role for the pack and an advisor to the alpha. The delta is the third level, and omega is the last level category in the hierarchy. The delta dominates omega but submits to betas and alphas. Scouts, hunters, elders, caretakers, and sentinels belong to the delta category. As omegas are ranked on the last level, they always have to submit to other dominant wolves in the pack. The omega wolves play the scapegoat role and are lastly allowed to eat in the pack.

In addition to the grey wolves social hierarchy, they have another interesting behavior in their hunting process. The

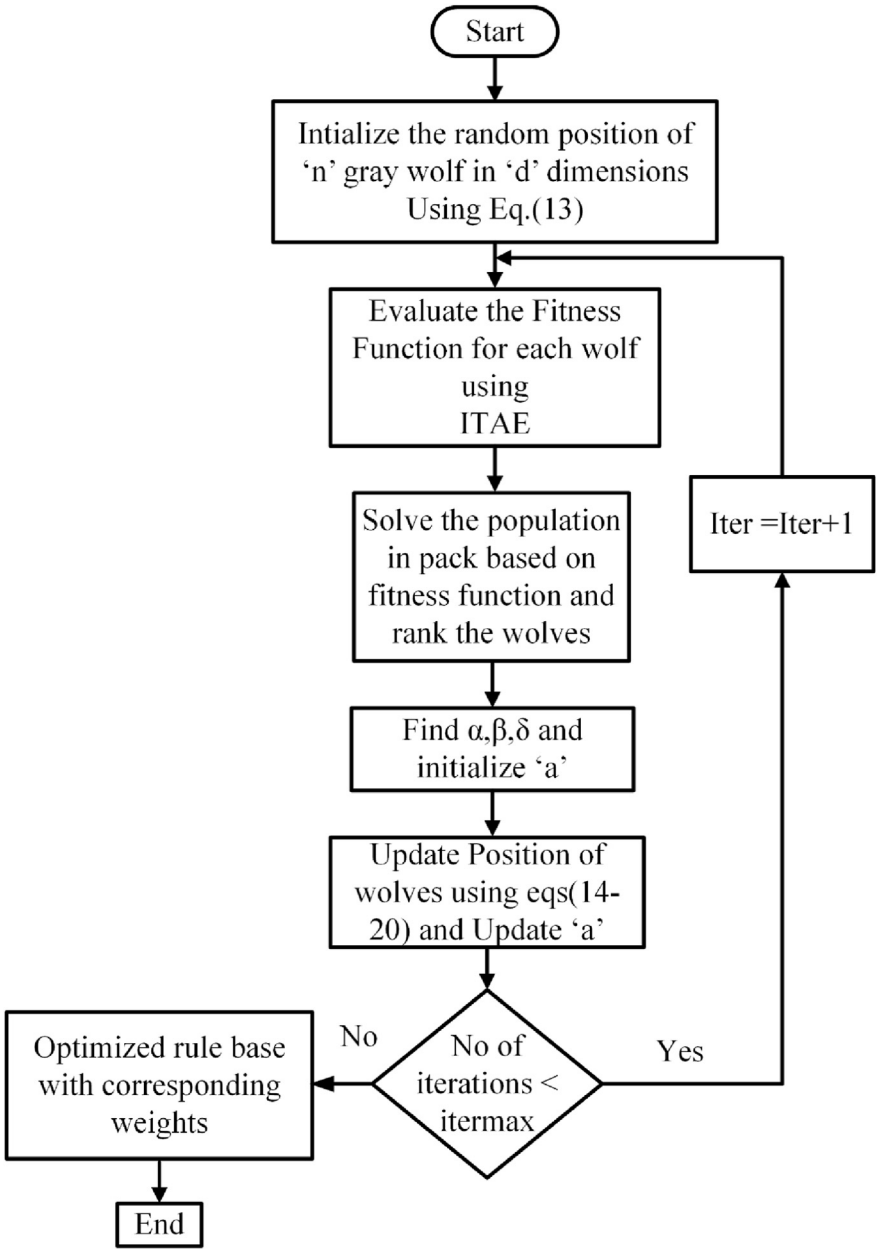

Fig. 10 – Flow chart of GWO optimized scaling factors of FLC.

main steps involved in grey wolves hunting for prey are as follows:

a) Social hierarchy
b) Encircling prey
c) Hunting
d) Attacking prey

Social hierarchy

In this GWO optimization technique, the alpha (α) wolves are considered as the best solution in the pack. In the same way, the beta (β) category wolf is second best, and the delta (δ) category is considered as the third-best solution. The leftover candidate solutions are grouped as omega (ω) wolves. In this GWO, the wolves α, β, and δ guide the hunting (optimization) process, and the omega wolves always follow them.

Encircling prey

The following equations present the encircling grey wolves for prey during their hunt. Here n represents the current iteration. $\vec{X}$ and $\vec{X}_p$ are the positions of a grey wolf and prey, $\vec{A}$ and $\vec{C}$ represents the coefficients vectors.

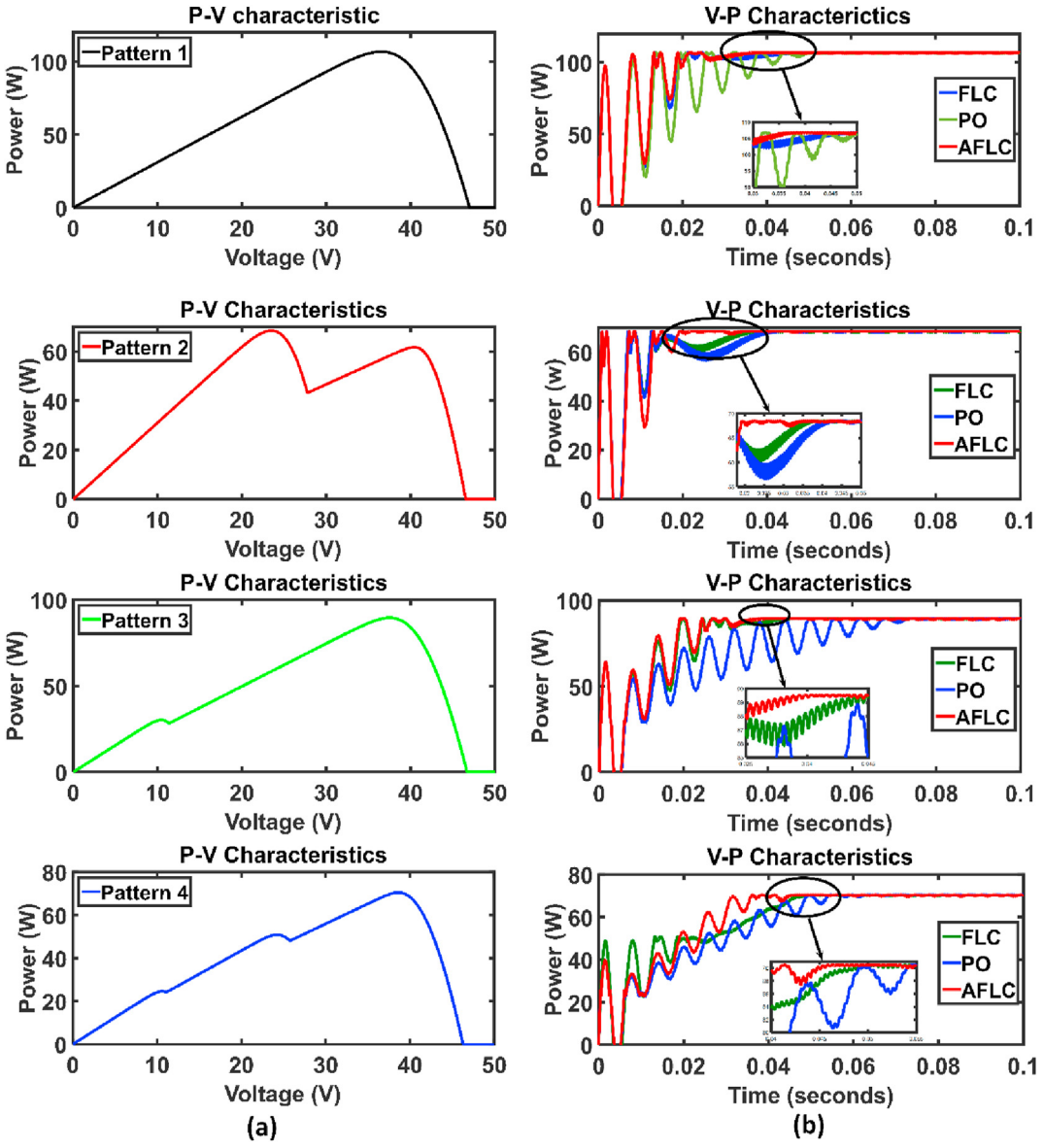

Fig. 11 – (a) V–P curves (b) The power output of SPVS for P&O, FLC, AFLC techniques for first, second, third, and fourth shading Patterns.

$$\vec{D} = \left| \vec{C}.\vec{X}_p^n - \vec{X}^n \right| \tag{13}$$

$$\vec{X}^{n+1} = \vec{X}^n + \vec{A}.\vec{D} \tag{14}$$

The coefficient vectors $\vec{A}$, $\vec{C}$ are obtained as:

$$\vec{A} = 2\vec{a}.\vec{r}_1 - \vec{a} \tag{15}$$

$$\vec{C} = 2.\vec{r}_2 \tag{16}$$

where $\vec{r}_1, \vec{r}_2$ are the random values in [0, 1], $\vec{a}$ is linearly varied from 2 to 0 based on iteration.

Hunting

Grey wolves have prey location recognizing ability and encircling them. In general, the hunt is guided by the alpha wolf, later beta and delta wolves join in the hunting process. In the mathematical model of grey wolves hunting behavior, all the search agents update their position based on the position of best candidate solution (α, β and δ). Grey wolves hunting behavior is follows as:

$$\vec{D}_\alpha = \left| \vec{C}_1.\vec{X}_\alpha - \vec{X} \right|;\ \vec{D}_\beta = \left| \vec{C}_1.\vec{X}_\beta - \vec{X} \right|;\ \vec{D}_\delta = \left| \vec{C}_1.\vec{X}_\delta - \vec{X} \right| \tag{17}$$

$$\vec{X}_1 = \vec{X}_\alpha - \vec{A}_1.\left(\vec{D}_\alpha\right);\ \vec{X}_2 = \vec{X}_\beta - \vec{A}_2.\left(\vec{D}_\beta\right);\ \vec{X}_3 = \vec{X}_\delta - \vec{A}_3.\left(\vec{D}_\delta\right) \tag{18}$$

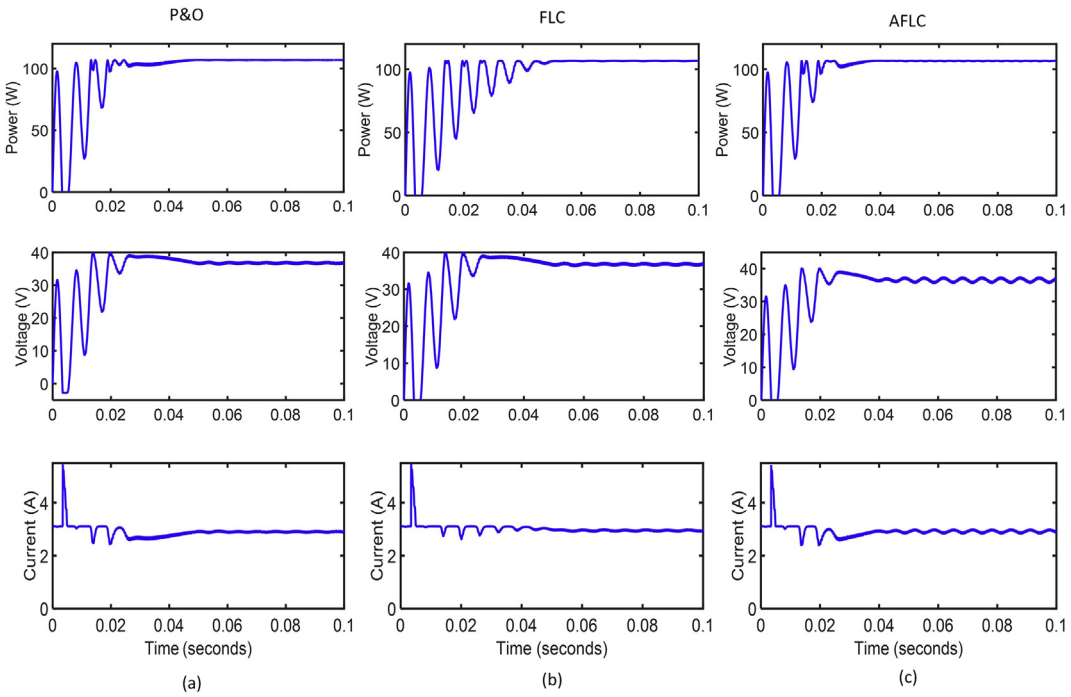

Fig. 12 – Simulated Power, Voltage and Current curves for shading pattern 1: 1.0, 1.0, 1.0 kW/m^2 (a) P&O based tracking, (b) FLC based tracking, and (c) Proposed AFLC based tracking.

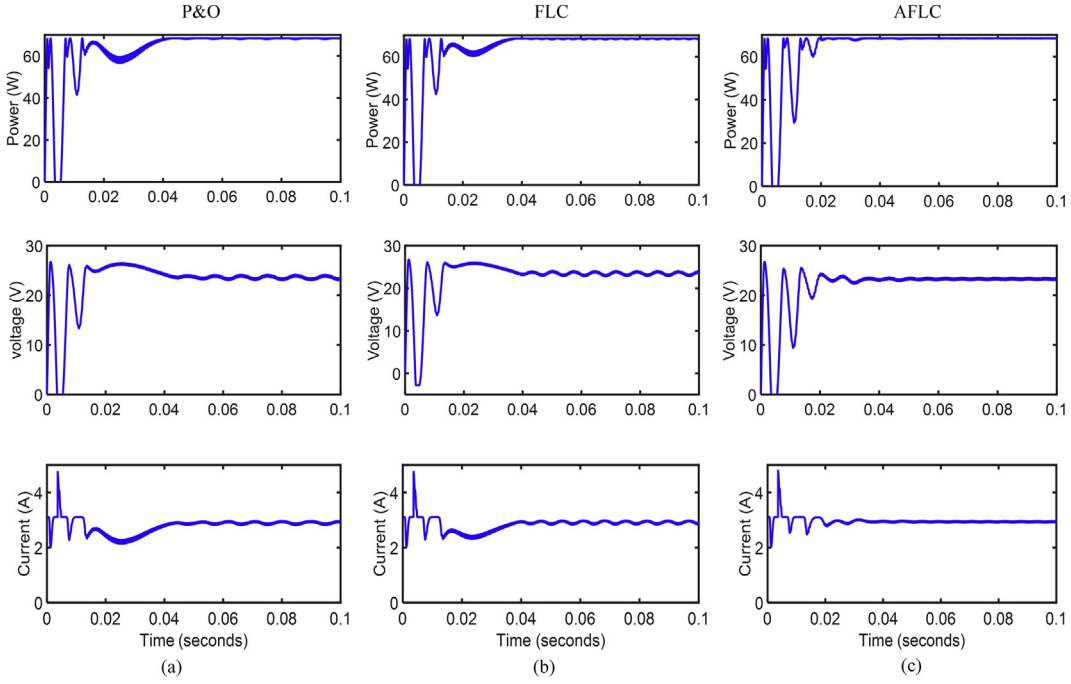

Fig. 13 – Simulated Power, Voltage and Current curves for shading pattern 2: 1.0, 1.0, 0.5 kW/m^2 (a) P&O based tracking, (b) FLC based tracking, and (c) Proposed AFLC based tracking.

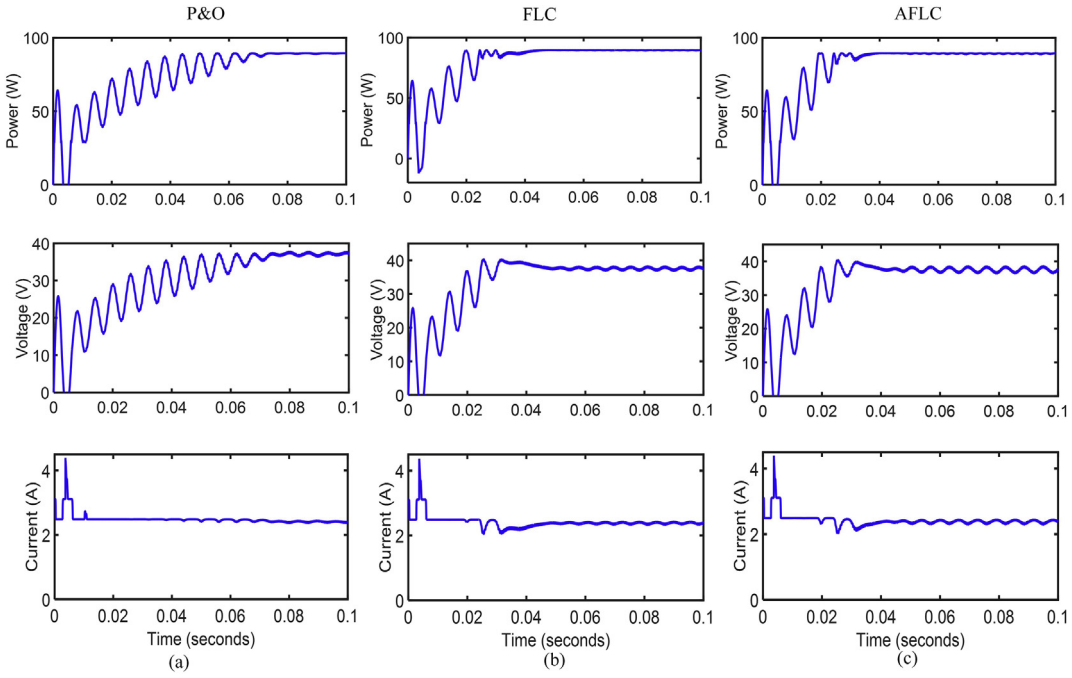

Fig. 14 – Simulated Power, Voltage and Current curves for shading pattern 3: 1.0, 0.8, 0.8 kW/m^2 (a) P&O based tracking, (b) FLC based tracking, and (c) Proposed AFLC based tracking.

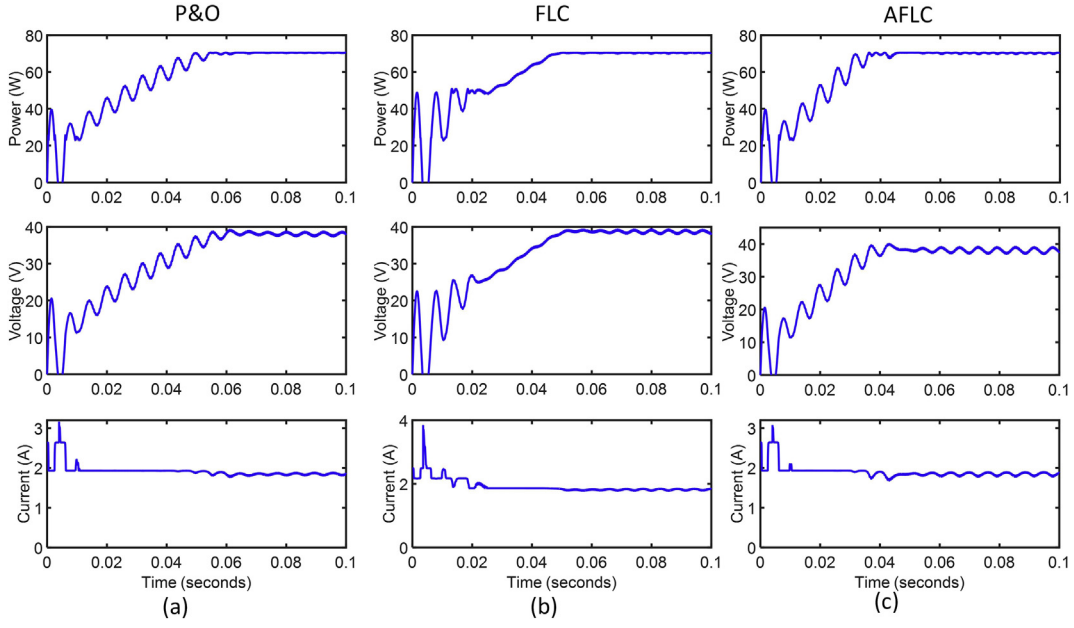

Fig. 15 – Simulated Power, Voltage and Current curves for shading pattern 4: 0.7.0, 0.8, 0.6 kW/m^2 (a) P&O based tracking, (b) FLC based tracking, and (c) Proposed AFLC based tracking.

$$\vec{X}^{n+1} = \frac{\vec{X}_1 + \vec{X}_2 + \vec{X}_3}{3} \tag{19}$$

Attacking prey

As stated above, the grey wolves hunting process finishes by attacking the prey when it stops moving. The value of $\vec{a}$ is linearly decreased from 2 to 0 in order to model the mathematical modeling of approaching the prey. Here the fluctuation range of $\vec{A}$ is decreases with $\vec{a}$. In the GWO algorithm, all

Table 2 – Quantitative Comparison of MPPT techniques.

Shading Pattern	Method	Power at MPP (W)	Voltage at MPP (V)	Current at MPP (A)	Tracking time (sec)	Maximum Power	Efficiency
Pattern1	P&O [16]	106.75	36.8	2.095	0.05	106.81	99.94
	FLC [21]	106.77	36.15	2.95	0.05		99.96
	AFLC [proposed]	106.78	36.5	2.92	0.038		99.97
Pattern2	P&O [16]	68.4	23.7	2.885	0.043	68.48	99.88
	FLC [21]	68.4	23.5	2.92	0.038		99.88
	AFLC [proposed]	68.43	23.3	2.94	0.035		99.92
Pattern3	P&O [16]	89.48	37.1	2.41	0.073	89.52	99.95
	FLC [21]	89.45	37.6	2.38	0.045		99.92
	AFLC [proposed]	89.5	37.7	2.37	0.04		99.97
Pattern4	P&O [16]	70.4	38.25	1.845	0.056	70.45	99.92
	FLC [21]	70.35	38.8	1.82	0.05		99.85
	AFLC[proposed]	70.42	38.2	1.84	0.046		99.95

Table 3 – A qualitative comparison of MPPT techniques.

Creteria	P&O	FLC	ACO-FLC [32]	Fuzzy-PSO [35]	Proposed GWO-FLC
Tracking speed	Slow	Moderate	Moderate	Moderate	Fast
Complexity	Less	Less	Moderate	Moderate	Less
Tracking efficiency	Less	Medium	Medium	Medium	High
Reliability	Low	Moderate	Low	High	High
Oscillations at MPP	High	Medium	moderate (constant oscillations at MPP)	High	Less
Tracking accuracy	Medium	Medium	Medium	Medium	Accurate

the search agents update their position to attack the prey based on the location of α, β, and δ wolves.

Search for prey

Grey wolves search based on the location of alpha, beta, and delta wolves. To search for the prey the grey wolves diverge from each other and converge while attacking the prey. The exploration behavior is emphasized when the random value $\vec{A}$ is greater than 1, or lesser than −1. This allows the GWO algorithm to globally search. In addition to $\vec{A}$, the GWO algorithm has another component favoring exploration is $\vec{C}$. The value of $\vec{C}$ randomly varies in [0 2]. When this component is greater than 1 the search agents are more attracted to the prey. This assists the GWO in favoring more exploration and avoidance of local optima.

GWO algorithm to tune the scaling factors of FLC parameters

The MPP tracking starts with an initial duty cycle. The input current I_{PV} and voltage V_{PV} of boost converter are measured to calculate the SPVS power $P_{PV}(k)$. Now, based on initial changes in power, the controller increases the duty cycle. At this stage, new I_{PV} and V_{PV} are measured to calculate new power P_{PV} (k+1). Based on present and past information of SPVS power, the controller decides to decrease or increase the duty cycle. This process of tracking continuous until the MPP reaches.

Fig. 10 depicts the flowchart of GWO based tuning of scaling factors of FLC Parameters. The sequential steps illustrated in Fig. 10 are summarized as follows:

Step 1: **Inialization:** Initialize the population size of GWO using the equation:

$$\vec{X}_{ij} = l\vec{b} + rand^{*}(u\vec{b} - l\vec{b}) \tag{20}$$

where, $l\vec{b} = [0\,0\,0\,0]$; $u\vec{b} = [1\,1\,1\,1]$;

The maximum iterations, number of control vectors, scaling factors, and position vectors are also initialized.

Step 2: **Fitness Evaluation:** Estimate fitness value of every individual wolf using Eq. (12)

Step 3: **Selection:** Rank the wolves in descending order according to their fitness value. Identify the best three wolves as α, β and δ in population.

Step 4: **Update the position of each wolf:** Update the wolf population positions using Eqs. (13)–(19).

Step 5: **Termination criteria:** If the termination criterion attains, record optimum scaling factors, else go for step 2.

Results and discussions

The time domain simulations for SPVS MPPT under four shading patterns is carried out using Matlab/Simulink. To illustrate the supremacy of Proposed AFLC technique, results are compared with FLC and conventional P&O methods. The performance of three MPPT methods is analyzed concerning tracking efficiency, tracking speed, and steady-state performance under each shading pattern. Four shading patterns, which includes different shading effects, were considered in the present work. The shading patterns considered to have different global MPP positions, such as first, second, and third peaks. The output power of SPVS for P&O, FLC, AFLC techniques under various irradiance patterns is depicted in Fig. 11.

Pattern 1: The solar irradiances for PV modules considered are 1.0, 1.0 and 1.0 kW/m^2. The V–P curve is depicted in Fig. 11(a) has only peaked with MPP of 106.81 W. Fig. 11 (b) illustrates the output power of SPVS using three MPPT techniques. From this figure, all the methods track GMPP with high efficiency. The total simulated results (power, voltage, and current) of SPVS for various MPPT techniques under this pattern are depicted in Fig. 12. AFLC and FLC achieve MPP with tracking time 0.038s and 0.05s. From the simulation results, it proves that the proposed AFLC decreases 24% tracking time compared to FLC.

Pattern 2: In this case, the solar irradiances for PV modules considered are 1.0, 1.0 and 0.5 kW/m^2. The V–P curve is depicted in Fig. 11(a). In this pattern, there are two peaks with MPP of 68.48 W and GMPP located at first peak. From Fig. 11 (b), all the techniques track GMPP with high efficiency. The total simulated results of SPVS for various MPPT techniques under this pattern are depicted in Fig. 13. AFLC and FLC achieve MPP with tracking time 0.035s, 0.038 and 0.043s and means that the proposed AFLC decreases 7.9% and 18.6% tracking time compared to FLC and P&O.

Pattern 3: For this, the solar irradiances of PV modules are 1.0, 0.8 and 0.8 kW/m^2. The V–P curve is depicted in Fig. 11(a). In this pattern, there are two peaks with MPP of 89.52 W and GMPP located at the second peak. The total simulation results of SPVS for various MPPT techniques under this pattern are depicted in Fig. 14. AFLC, FLC, and P&O achieve MPP with tracking time 0.04s, 0.045 and 0.073s. This means that the proposed AFLC decreases 11.12% and 45.1% tracking time compared to FLC and P&O.

Pattern 4: For this, the solar irradiances of PV modules are 0.7, 0.8, and 0.6 kW/m^2. The V–P curve is depicted in Fig. 11(a). In this pattern, there are three peaks with MPP of 70.45 W and GMPP located at third peak. The total simulation results of SPVS for various MPPT techniques under this pattern are depicted in Fig. 15. AFLC, FLC, and P&O achieve MPP with tracking time 0.046s, 0.05 and 0.056s. This means that the proposed AFLC decreases 8% and 17.9% tracking time compared to FLC and P&O. A comparative study of different MPPT methods is itemized in Table 2. From this table, it shows that the superiority of AFLC based tracking among the FLC and P&O.

The GWO optimized FLC MPPT performance evaluation with other established methods stated in literature has been presented in Table 3. The proposed MPPT technique has high tracking efficiency, reduced oscillations at MPP, fast-tracking speed, and more reliable compared to the traditional FLC and P&O methods. In comparison with the Ant colony optimized (ACO) fuzzy controller discussed in Ref. [32], the proposed GWO optimized FLC MPPT tracks MPP with fast-tracking speed and fewer oscillations. Additionally, the complexity with ACO-FLC MPPT is more due to more algorithmic parameters which may lead to converging at local best. In the Fuzzy-PSO [35], the PSO algorithm is used to adjust the scaling factors of MFs of FLC to track global MPP. But the PSO algorithm has slow convergence because of the more number of parameters to be initialized (r1, r2, c1, c2), and it may lead to divergence with the improper selection of initialization parameters. Hence, the PSO requires more computational time compared to Grey wolf optimization. Therefore, the proposed GWO optimized FLC MPPT has a fast-tracking speed, fewer oscillations, and fast response under partial shading conditions.

Conclusion

In this paper, an adaptive fuzzy based MPPT technique is proposed for smooth and efficient tracking under partial shading conditions. Four shading patterns are employed to experiment with the performance of the proposed AFLC controller. The comparative studies and the evaluations confirmed that the proposed controller obtains a trade-off solution between low oscillations and high tracking speed while compared with other controllers in literature. In particular, the proposed controller shows its supremacy in tracing over the P&O method and the fuzzy method under the various partial shading conditions. Moreover, the proposed AFLC controller does not require the complete mathematical model of the system. Hence it will be a solution under the challenging environmental conditions for the PV systems.

Declaration of competing interest

The authors declare that they have no known competing financial interests or personal relationships that could have appeared to influence the work reported in this paper.

REFERENCES

[1] Mekhilef S, Saidur R, Safari A. A review on solar energy use in industries. Renew Sustain Energy Rev 2020;15(4):1777–90.
[2] Harrabi Naziha, Souissi Mansour, Abdel Aitouche, Mohamed Chaabane. Modeling and control of photovoltaic and fuel cell based alternative power systems. Int J Hydrogen Energy 2018;43(25):11442–51. https://doi.org/10.1016/j.ijhydene.2018.03.012. ISSN 0360-3199.
[3] Bader Alajmi N, Khaled Ahmed H. A maximum power point tracking technique for partially shaded photovoltaic systems in microgrids. IEEE Trans Ind Electron April 2013;60(4):1596–606.
[4] Guerrero JM, Blaabjerg F, Zhelev T, Hemmes K, Monmasson E, Jemei S, Comech MP, Granadino R, Frau JI. Distributed generation: toward a new energy paradigm. IEEE Ind. Electron. Mag. Mar. 2010;4(1):52–64.
[5] Ahmed KH, Massoud AM, Finney SJ, Williams BW. A modified stationary reference frame-based predictive current control with zero steady-state error for LCL coupled inverter-based distributed generation systems. IEEE Trans Ind Electron Apr. 2011;58(4):1359–70.
[6] Liserre M, Sauter T, Hung JY. Future energy systems: integrating renewable energy sources into the Smart power grid through industrial electronics. IEEE Ind.Electron. Mag. Mar. 2010;4(1):18–37.
[7] Carrasco JM, Franquelo LG, Bialasiewicz JT, Galvan E, Guisado RCP, Prats MAM, Leon JI, Moreno-Alfonso N. Power electronic systems for the grid integration of renewable energy sources: a survey. IEEE Trans Ind Electron Jun. 2006;53(4):1002–16.
[8] Ishaque Kashif, Zainal Salam, Amir Shamsudin, Amjad Muhammad. A direct control based maximum power

point tracking method for photovoltaic system under partial shading conditions using particle swarm optimization algorithm. Appl Energy June 2012;99:414–22.
[9] N. A. Rahim, M. F. Mohammed and B. M. Eid, "Assessment of effect of haze on photovoltaic systems in Malaysia due to open burning in Sumatra," in IET Renew Power Gener, vol. 11, no. 3, pp. 299-304, 22 2 2017, doi: 10.1049/iet-rpg.2016.0069.
[10] Abatzoglou John T, Williams A Park. Impact of anthropogenic climate change on wildfire across western US forests. Proc Natl Acad Sci Unit States Am Oct 2016;113(42):11770–5. https://doi.org/10.1073/pnas.1607171113.
[11] Gao Manyi, Yang Weiwei, Yu Yongsheng. Monodisperse PtCu alloy nanoparticles as highly efficient catalysts for the hydrolytic dehydrogenation of ammonia borane. Int J Hydrogen Energy 2018;43(31):14293–300. https://doi.org/10.1016/j.ijhydene.2018.05.158. ISSN 0360-3199.
[12] Hu Liu, Liu Xinyang, Yang Weiwei, Shen Mengqi, Geng Shuo, Yu Chao, Shen Bo, Yu Yongsheng, ". Photocatalytic dehydrogenation of formic acid promoted by a superior PdAg@g-C3N4 Mott–Schottky heterojunction. J Mater Chem A 2019;7:2022. https://doi.org/10.1039/c8ta11172c.
[13] Wang Yingjun, Bao Shuangyou, Liu Yequn, Yang Weiwei, Yu Yongsheng, Ming Feng, Li Kefei. Efficient photocatalytic reduction of Cr(VI) in aqueous solution over CoS2/g-C3N4-rGO nanocomposites under visible light. Appl Surf Sci 2020;510:145495. https://doi.org/10.1016/j.apsusc.2020.145495. ISSN 0169-4332.
[14] Patel H, Agarwal V. Matlab-based modeling to study the effects of partial shading on PV array characteristics. IEEE Trans Energy Convers Mar. 2008;23(1):302–10.
[15] Lijun G, Dougal RA, Shengyi L, Iotova AP. Parallel-connected solar PV system to address partial and rapidly fluctuating shadow conditions. IEEE Trans Ind Electron May 2009;56(5):1548–56.
[16] Esram T, Chapman PL. Comparison of photovoltaic array maximum power point tracking techniques. IEEE Trans Energy Convers Jul. 2007;22(2):439–49.
[17] Fangrui L, Yong K, Yu Z, Shanxu D. Comparison of P&O and hill climbing MPPT methods for grid-connected PV converter. SAVE Proc 2008;3rd*ICIEA*:804–7.
[18] Kimball JW, Krein PT. Discrete-time ripple correlation control formaximum power point tracking. IEEE Trans Power Electron Sep. 2008;23(5):2353–62.
[19] Ozdemir S, Altin N, Sefa I. Fuzzy logic based MPPT controller for high conversion ratio quadratic boost converter. Int J Hydrogen Energy 2017:1–12.
[20] Abdullah M. Noman, Khaled E. Addoweesh, and Hussein M. Mashaly, "A fuzzy logic control method for MPPT of PV systems," 38th annual conference on IEEE industrial electronics society (IECON),25-28 oct. 2012, montreal, QC, Canada, DOI: 10.1109/IECON.2012.6389174.
[21] Al-Majidi Sadeq D, Abbod Maysam F, Al-Raweshidy Hamed S. A novel maximum power point tracking technique based on fuzzy logic for photovoltaic systems. Int J Hydrogen Energy 2018;43(31):14158–71. https://doi.org/10.1016/j.ijhydene.2018.06.002. ISSN 0360-3199.
[22] Jaw-KuenShiau Yu-Chen Wei, Chen Bo-Chih. A study on the fuzzy-logic-based solar power MPPT algorithms using different fuzzy input variables. Algorithms 2015;8:100–27.
[23] Bendib B, Krim F, Belmili H, Almi MF, Boulouma S. Advanced fuzzy MPPT controller for a stand-alone PV system. Energy Procedia 2014;50:383–92.
[24] Bounechba H, Bouzid A, Nabti K, Benalla H. Comparison of perturb & observe and fuzzy logic in maximum power point tracker for PV systems. Energy Procedia 2014;50:677–84.
[25] C. S. Chin, P. Neelakantan, H. P. Yoong, and K. T. K. Teo, "Fuzzy logic based MPPT for photovoltaic modules influenced by solar irradiation and cell temperature,"13thInternational conference on computer modelling and simulation, 30 march-1 april 2011, cambridge, UK, DOI: 10.1109/UKSIM.2011.78.
[26] Mahamudul Hasan, Saad Mekhilef, Ibrahim Henk Metselaar. Photovoltaic system modeling with fuzzy logic based maximum power point tracking algorithm. Int J Photoenergy 2013;2013. https://doi.org/10.1155/2013/762946. Article ID 762946.
[27] Gheibi Amir, Mohammadi SMA, maghfoori M. Maximum power point tracking of photovoltaic generation based on the type 2 fuzzy logic control method. Energy Procedia 2011;12:538–46.
[28] Ankit Gupta, Pawan Kumar, Rupendra Kumar Pachauri, and Yogesh K. Chauhan, "Performance analysis of neural network and FuzzyLogic based MPPT techniques for solar PV systems," 6th IEEE power India international conference (PIICON),5-7 dec. 2014, Delhi, India, DOI: 10.1109/POWERI.2014.7117722.
[29] Bellia Habbati, Youcef Ramdani, Fatima Moulay. "A detailed modeling of photovoltaic module using MATLAB". NRIAG J Astron Geophys 2014;3:53–61. https://doi.org/10.1016/j.nrjag.2014.04.001.
[30] Bhukya L, Srikanth N. "A novel photovoltaic maximum power point tracking technique based on grasshopper optimized fuzzy logic approach". Int J Hydrogen Energy 2020;45(16):9416–27.
[31] AnilKumar A, Srikanth NV. Load frequency control for diverse sources of interconnected two area power system: an adaptive fuzzy approach. ICCCCM), Allahbad. In: 2016 international conference on control, computing, communication and materials; 2016. p. 1–4. https://doi.org/10.1109/ICCCCM.2016.7918218.
[32] M. Adly, and A.H. Besheer, "An optimized fuzzy maximum power point tracker for stand alone photovoltaic systems: Ant colony approach," 7th IEEE conference on industrial electronics and applications (ICIEA), 18-20 july 2012, Singapore, DOI: 10.1109/ICIEA.2012.6360707.
[33] Jouda Arfaoui, Elyes Feki, Rabhi Abdel hamid, Abdel kader Mami. "Optimization of scaling factors of fuzzy–MPPT controller for stand-alonePhotovoltaic system by particle swarm optimization. Energy Procedia 2017;111:954–63.
[34] Larbes C, Cheikh SMA, Obeidi T, Zerguerras A. Genetic algorithms optimized fuzzy logic control for the maximum power pointtracking in photovoltaic system. Renew Energy 2009;34:2093–100.
[35] Soufi Y, Bechouat M, Kahla S. Fuzzy-PSO controller design for maximum power point tracking in photovoltaic system. Int J Hydrogen Energy 2016;42(13):8680–8.
[36] Mirjalili S, Mirjalili SM, Lewis A. Grey wolf optimizer, vol. 69. Proc. Elsevier; 2014. p. 46–61.